PAR proteins direct asymmetry of the cell cycle regulators Polo-like kinase and Cdc25

David M. Rivers, Sergio Moreno, Mary Abraham, and Julie Ahringer

The Gurdon Institute and Department of Genetics, University of Cambridge, Cambridge CB2 1QN, England, UK

Cell cycle lengths vary widely among different cells within an animal, yet mechanisms of cell cycle length regulation are poorly understood. In the *Caenorhabditis elegans* embryo, the first cell division produces two cells with different cell cycle lengths, which are dependent on the conserved partitioning-defective (PAR) polarity proteins. We show that two key cell cycle regulators, the Polo-like kinase PLK-1 and the cyclin-dependent kinase phosphatase CDC-25.1, are asymmetrically distributed in early embryos. PLK-1 shows anterior cytoplasmic enrichment and CDC-25.1 shows PLK-1–dependent enrichment in the anterior nucleus. Both proteins are required for normal mitotic progression. Furthermore, these asymmetries are controlled by PAR proteins and the muscle excess (MEX) proteins MEX-5/MEX-6, and the latter is linked to protein degradation. Our results support a model whereby the PAR and MEX-5/MEX-6 proteins asymmetrically control PLK-1 levels, which asymmetrically regulates CDC-25.1 to promote differences in cell cycle lengths. We suggest that control of Plk1 and Cdc25 may be relevant to regulation of cell cycle length in other developmental contexts.

Introduction

During development, cell cycle lengths vary for different cell types, and this is important for the determination of their fates and functions. Misregulation of cell cycle length can cause unregulated growth, abnormal cell fates, gastrulation defects, and other developmental abnormalities and diseases. The *Caenorhabditis elegans* embryo is an excellent organism for studying differential regulation of cell cycle length because the first division produces daughters with different cell cycle timing (Deppe et al., 1978; Sulston et al., 1983). This asynchrony is controlled by the partitioning-defective (PAR) proteins, conserved cell polarity regulators that establish and maintain cell polarity in most animal cells (Kemphues et al., 1988; Watts et al., 1996, 2000; Morton et al., 2002; Schneider and Bowerman, 2003; Nance, 2005). Some PAR proteins have also been implicated in proliferation control. For example, the serine/threonine kinase PAR-4 is homologous to the human tumor suppressor LKB1, which is mutated in Peutz-Jegher syndrome (McGarrity and Amos, 2006). An important open question is how cell polarity influences cell cycle timing.

The first cell division of *C. elegans* is asymmetric and produces a larger AB cell and a smaller P1 cell. Cell division at the two-cell stage is asynchronous, with AB dividing 2 min before P1. These asymmetries, as well as the asymmetric distribution of cytoplasmic and cortical components, are controlled by the PAR polarity proteins (Schneider and Bowerman, 2003; Nance, 2005). For five of the six *par* genes, mutation results in loss of both size asymmetry and of asynchrony of cell division (Kemphues et al., 1988; Watts et al., 1996; Morton et al., 2002). However, differential control of cell cycle timing appears to be independent of cell size because *par-4* mutant embryos have synchronous AB and P1 divisions despite retaining the size asymmetry (Watts et al., 2000). This suggests that the polarity machinery may regulate the asynchronous second division directly, although the specific mechanism remains elusive.

Other factors likely to be involved in cell cycle asynchrony are the muscle excess (MEX) proteins MEX-5 and MEX-6 and the DNA replication checkpoint. MEX-5 and MEX-6 control asymmetric protein degradation downstream of the PAR proteins, and their loss leads to AB and P1 dividing synchronously (Piano et al., 2002). Interference with the DNA replication checkpoint affects P1 cell cycle length more than that of AB (Encalada et al., 2000; Brauchle et al., 2003; Kalogeropoulos et al., 2004). However, much of the difference between AB and P1 cell cycle lengths is independent of the replication checkpoint, which strongly suggests the involvement of other yet to be determined regulatory factors.

Correspondence to J. Ahringer: ja219@cam.ac.uk

S. Moreno's permanent address is Centro de Investigacion del Cancer, Consejo Superior de Investigaciones Científicas, Campus Miguel de Unamuno, University of Salamanca, 37007 Salamanca, Spain.

Abbreviations used in this paper: MEX, muscle excess; NEBD, nuclear envelope breakdown; PAR, partitioning defective.

The online version of this paper contains supplemental material.

The Journal of Cell Biology
http://www.jcb.org/cgi/doi/10.1083/jcb.200710018

Supplemental Material can be found at:
http://www.jcb.org/cgi/content/full/jcb.200710018/DC1

One possible mechanism for achieving different cell cycle lengths in AB and P1, compatible with known PAR protein functions, is the differential localization of core cell cycle regulatory components. Using a candidate approach to test this hypothesis, we found that both the Polo-like kinase PLK-1 and the Cdk phosphatase CDC-25.1 show enrichments in AB cells and that the polarity machinery controls these asymmetries. Both PLK-1 and CDC-25.1 promote cell cycle progression and PLK-1 is required for normal levels of nuclear CDC-25.1. These findings suggest a regulatory mechanism whereby the polarity machinery directs the asynchrony of the second division through the asymmetric distribution of PLK-1 and CDC-25.1 in the *C. elegans* embryo.

Results and discussion

The Cdk phosphatase CDC-25.1 is enriched in AB nuclei and required for cell division timing

Previous studies have shown that AB and P1 spend an equivalent length of time in mitosis, indicating that regulation of cell division asynchrony occurs before the onset of nuclear envelope breakdown (NEBD) in AB (Encalada et al., 2000; Brauchle et al., 2003). We postulated that a possible mechanism could be asymmetric distribution of key cell cycle regulators. Taking a candidate approach, we looked at the subcellular localization pattern of two cell cycle regulatory components, the E-type cyclin CYE-1 and the Cdk phosphatase CDC-25.1.

Nuclear localization of cyclin E demarcates and has been shown to be required for the initiation of S phase in mammalian cells (Moroy and Geisen, 2004). We used nuclear localization of the sole *C. elegans* cyclin E protein CYE-1 as a marker for assessing the time of onset of S phase in AB and P1 cells (Brodigan et al., 2003). We found that CYE-1 can be detected in the future AB and P1 nuclei at equal levels as nuclei begin to reform in the first telophase (Fig. 1 A). This symmetric nuclear distribution persists throughout the two-cell stage up to NEBD of AB. Therefore, as gauged by CYE-1 localization, the onset of S phase appears to be synchronous. This agrees with previous data showing synchronous S phase initiation in AB and P1 by DAPI staining (Edgar and McGhee, 1988).

The dual specificity Cdc25 family of phosphatases (Cdc25A, B, and C) activates Cdk–cyclin complexes to promote cell cycle progression (Brodigan et al., 2003; Busino et al., 2004). The temporal activation of Cdk–cyclin activity has been shown to be dependent on regulated nuclear import/export of Cdc25 proteins (Karlsson et al., 1999; Toyoshima-Morimoto et al., 2002). There are four Cdc25 homologues in *C. elegans* (Ashcroft et al., 1998). We focused on one, CDC-25.1, because it is the only one essential for normal meiosis and embryonic mitosis (Ashcroft et al., 1999). Although its precise roles and distribution have not yet been investigated, CDC-25.1 localizes to the nuclei of early embryos (Ashcroft et al., 1999). Intriguingly, we found that soon after CDC-25.1 is detectable in AB and P1 nuclei, there is an asymmetric distribution. In early two-cell embryos, where DNA condensation has yet to occur, we observed enrichment of CDC-25.1 in AB nuclei in 10/12 embryos (Fig. 1 B). This asymmetric nuclear enrichment persists until NEBD in AB and is apparent in all two-cell embryos where DNA condensation has begun ($n = 18$; Fig. 1 B). The greater abundance of CDC-25.1 in AB compared with P1 is consistent with a role in promoting an earlier cell division time.

If CDC-25.1 regulates asynchronous cell cycle timing at the two-cell stage, we would still expect it to promote cell division in both AB and P1. To test this possibility, we knocked down *cdc-25.1* in wild-type embryos by RNAi and assessed cell cycle timing of both AB and P1 by video microscopy. Previous studies have shown that strong RNAi knockdown of *cdc-25.1* results in severe meiotic defects (Ashcroft et al., 1999). To overcome this obstacle, we performed a weaker RNAi of *cdc-25.1* by feeding adult worms RNAi bacteria for a shorter period of time (see Materials and methods). Under these conditions, embryos still failed to hatch but they completed meiosis and we could assay cell division timing at the two-cell stage. Cell cycle times of wild-type and *cdc-25.1(RNAi)* embryos were measured from the onset of NEBD in P0 to NEBD in AB and P1. Although the cell cycle lengths for wild-type AB and P1 were 14.4 ± 0.26 and 16.6 ± 0.28 min, respectively ($n = 9$), both were lengthened in the *cdc-25.1*-depleted embryos (18.1 ± 0.58 and 22.8 ± 0.80 min, respectively; $n = 5$; Fig. 2 A and Table S1 A, available at http://www.jcb.org/cgi/content/full/jcb.200710018/DC1). In one case, we observed a synchronous division of AB and P1 at 22.2 min, which is consistent with previous observations (Ashcroft et al., 1999). These findings show that CDC-25.1 positively regulates the timing of cell division in AB and P1.

Most embryos partially depleted for *cdc-25.1* still show asynchronous cell division. However, we observed that the mean time between AB and P1 divisions in *cdc-25.1*-depleted embryos is lengthened compared with wild-type embryos (4.7 vs. 2.2 min, respectively). The greater sensitivity of P1 to CDC-25.1 depletion suggests that CDC-25.1 protein levels may play an important role in cell cycle length. The *cdc-25(RNAi)* loss-of-function phenotypes, together with the asymmetry of nuclear CDC-25.1, are consistent with a model whereby the timing of division in the two-cell embryo is controlled by regulating nuclear levels of CDC-25.1.

The rate of nuclear CDC-25.1 accumulation is asynchronous in AB and P1

The asymmetric nuclear localization of CDC-25.1 is the earliest identified marker of asynchronous cell division. To better understand the dynamics of CDC-25.1 nuclear accumulation, we generated a transgenic strain expressing GFP::CDC-25.1 and examined its localization in AB and P1 nuclei (see Materials and methods). Similar to endogenous CDC-25.1, GFP::CDC-25.1 nuclear levels become asymmetric in early two-cell embryos soon after detection in the nuclei. By comparing normalized fluorescence intensities of GFP::CDC-25.1 in AB and P1 nuclei over time, we found that AB accumulates nuclear CDC-25.1 at a faster rate than P1 (Fig. 3 A and Video 1, available at http://www.jcb.org/cgi/content/full/jcb.200710018/DC1). The maximal rate difference of GFP::CDC-25.1 nuclear accumulation in AB versus P1 is 3.9 ± 1.0 ($n = 4$). To further verify that the difference in nuclear CDC-25.1 levels is caused by active differential regulation in AB compared with P1, we simultaneously

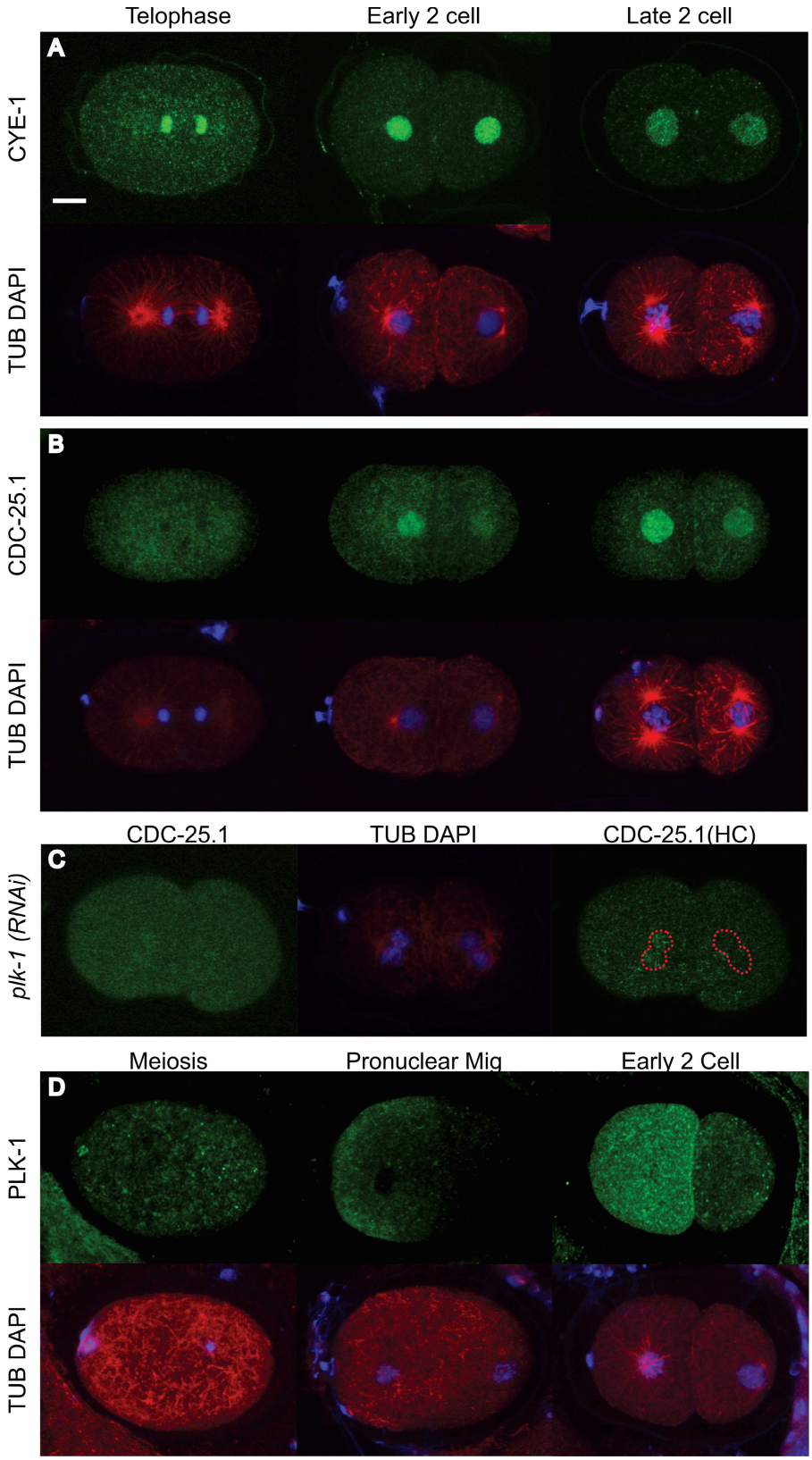

Figure 1. **Localization of CYE-1, CDC-25.1, and PLK-1 in wild-type embryos.** (A and B) CYE-1 (A) and CDC-25.1 (B) immunostaining (green) is shown on top; costaining of DNA (DAPI, blue) and tubulin (red) is shown on the bottom. CYE-1 is found at equal levels in AB and P1 nuclei; AB nuclei show higher levels of CDC-25.1 than P1 nuclei from the early two-cell stage onward. (C) The *plk-1(RNAi)* embryo has reduced nuclear level of CDC-25.1 compared with the wild type but retains asymmetry of distribution (right, high contrast [HC] image; dotted line marks nuclear envelope). (D) PLK-1 is shown on top (green); DNA (DAPI, blue) and tubulin (red) are shown on the bottom. Anterior cytoplasmic enrichment of PLK-1 is observed from pronuclear migration onwards. Bar, 10 μm.

photobleached AB and P1 nuclear GFP::CDC-25.1 in early two-cell embryos and measured the fluorescence recovery in the nuclei over time. Similar to our observations with the unbleached GFP::CDC-25.1, the maximal rate difference of GFP::CDC-25.1 nuclear recovery in AB was significantly greater than in P1 (2.7 ± 0.4-fold higher; $n = 5$; Fig. 3 B).

We also observed that AB nuclei show a higher level of GFP::CDC-25.1 than P1 nuclei at comparable cell cycle times

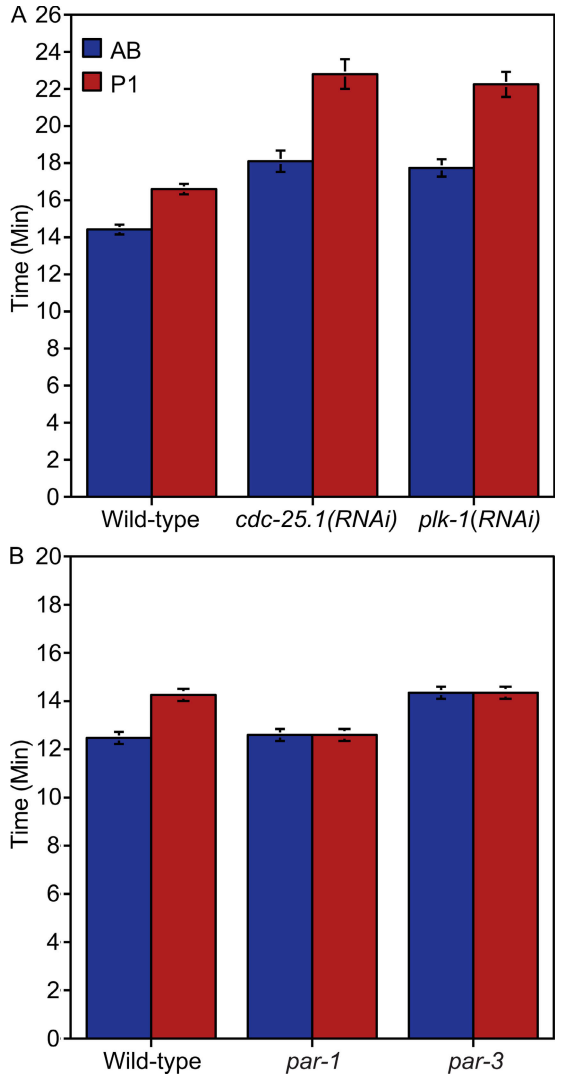

Figure 2. **Cell cycle timings in *cdc-25.1(RNAi)*, *plk-1(RNAi)*, *par-1*, and *par-3* embryos.** Mean cell cycle times ± SEM from the onset of NEBD in P0 to the onset of NEBD in AB or P1. Corresponding p-values are given in Table S1 (A and B, available at http://www.jcb.org/cgi/content/full/jcb.200710018/DC1). (A) *cdc-25.1(RNAi)* and *plk-1(RNAi)* embryos have lengthened AB and P1 cell cycle times. (B) P1 cell cycle time is shortened in *par-1* mutant embryos, whereas AB cell cycle time is lengthened in *par-3* mutant embryos.

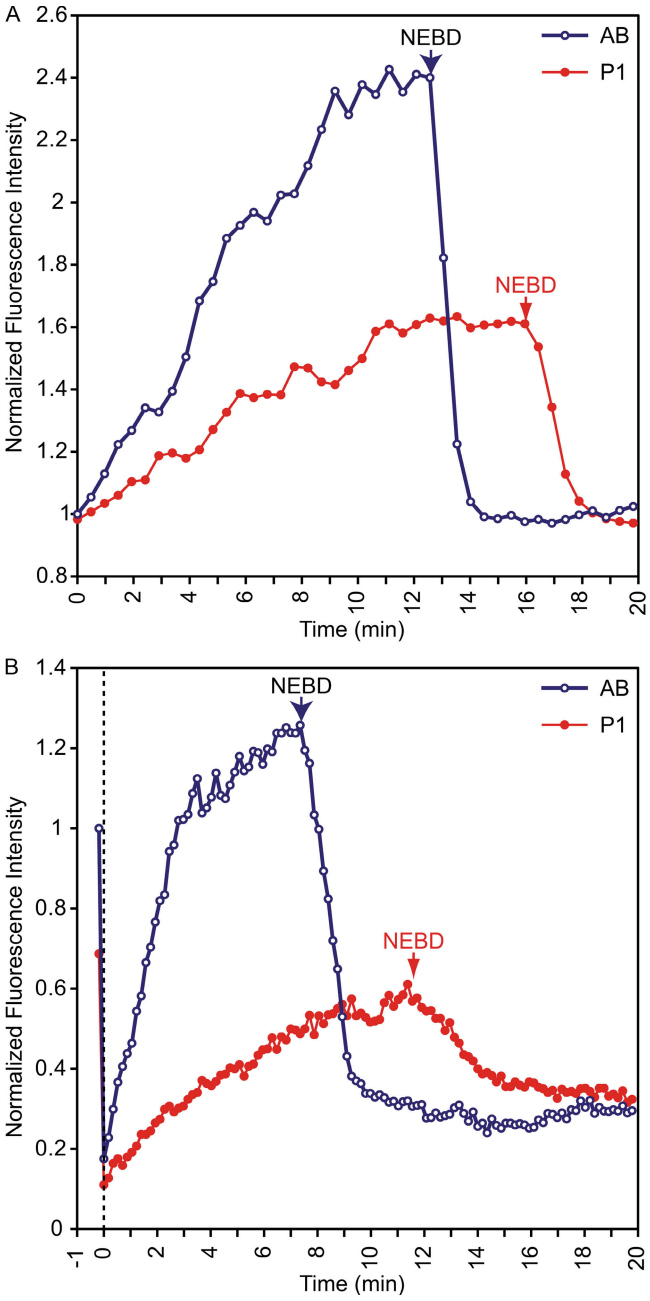

Figure 3. **Rate of GFP::CDC-25.1 nuclear accumulation is higher in AB than in P1.** Plots show normalized nuclear fluorescence intensities of *Ppie-1*::GFP::CDC-25.1 in AB and P1 through time during the second cell cycle. Initial fluorescence in AB nucleus was arbitrarily set to 1. (A) Plot from representative GFP::CDC-25.1 embryo ($n = 5$). (B) Plot from representative GFP::CDC-25.1 FRAP experiment ($n = 5$). AB and P1 nuclei were simultaneously photobleached at 0 min.

(Fig. 3 A and Video 2, available at http://www.jcb.org/cgi/content/full/jcb.200710018/DC1). Indeed, nuclear levels of GFP::CDC-25.1 are distinctly higher in AB nuclei than in P1 nuclei before NEBD (Fig. 3). These results indicate that the rate of nuclear CDC-25.1 accumulation is asymmetrically regulated in AB and P1, and this might lead to the difference in overall levels. We note that the difference in nuclear CDC-25.1 levels in AB compared with P1 at NEBD suggests that the absolute amount of CDC-25.1 is not the sole determinant of mitotic entry time.

The Polo-like kinase PLK-1 is anteriorly enriched and required for cell division timing

Previous studies in HeLa cells have shown that the Polo-like kinase Plk1 phosphorylates Cdc25C to promote its nuclear accumulation and the subsequent entry into mitosis (Toyoshima-Morimoto et al., 2002). If PLK-1 similarly regulates CDC-25.1 in *C. elegans*, then loss of *plk-1* should affect AB and P1 cell cycle lengths in a manner similar to that of loss of *cdc-25.1*. Previous RNAi loss-of-function studies with *plk-1* resulted in a strong one-cell arrest phenotype caused by a failure in cytokinesis (Chase et al., 2000). Therefore, as we did with *cdc-25.1*, we generated embryos with a weak loss of *plk-1* function by carrying our RNAi for shorter periods then and assessing cell cycle lengths in AB and P1. We found that *plk-1(RNAi)* embryos, like *cdc-25.1(RNAi)*

embryos, show longer AB and P1 cell cycle times: 17.7 ± 0.47 and 22.2 ± 0.68 min, respectively, as well as an increase in the difference between AB and P1 division time to 4.5 min (n = 16; Fig. 2 A and Table S1 A). We next investigated whether *C. elegans* PLK-1 regulates endogenous nuclear CDC-25.1 levels. In wild-type embryos, nuclear fluorescence is higher in AB than in P1 (Fig. 1 B; and see Fig. 5 B). We found that *plk-1(RNAi)* embryos show reduced nuclear CDC-25.1 fluorescence in both AB and P1 without a reduction in cytoplasmic levels; however, nuclear levels remain asymmetric (Figs. 1 C and S1 C, available at http://www.jcb.org/cgi/content/full/jcb.200710018/DC1). These results suggest that PLK-1 plays a role in promoting CDC-25.1 nuclear accumulation.

To further investigate a role for PLK-1 in the regulation of asynchronous cell cycle timing, we looked at its localization in early embryos. Strikingly, PLK-1 is enriched in the anterior cytoplasm of the one-cell embryo (Fig. 1 D; noted in Sumiyoshi et al., 2002). PLK-1 distribution is uniform at meiosis (n = 8) and then becomes asymmetric by pronuclear migration (n = 6; Fig. 1 D). From metaphase of P0 to the end of the two-cell stage, all embryos continue to show anterior enrichment of PLK-1 (n = 56; Fig. 1 D). As previously shown, we also observed PLK-1 localization to centrosomes and metaphase chromosomes (Chase et al., 2000). The anterior cytoplasmic enrichment places PLK-1 at the right place and time to promote greater CDC-25.1 nuclear accumulation in AB than in P1.

To summarize, PLK-1 shows anterior cytoplasmic enrichment, PLK-1 is required for nuclear accumulation of CDC-25.1, and both PLK-1 and CDC-25.1 promote cell cycle progression. These data support a model whereby the asymmetric localization of PLK-1 in the anterior cytoplasm of the one cell embryo leads to an increased rate of CDC-25.1 nuclear accumulation in AB and therefore to an earlier entry into mitosis of AB compared with P1.

PAR proteins and MEX-5/MEX-6 control PLK-1 and CDC-25.1 asymmetries

PAR proteins control overall embryonic polarity, including the size asymmetry of the first division, protein distribution asymmetries, and the asynchronony of the second division (Gönczy and Rose, 2006). To ask whether PAR proteins might control cell division timing differences through regulation of PLK-1 and CDC-25.1 asymmetries, we examined their patterns of localization in *par-1*, *-2*,- *3*, and *-4* mutants. Indeed, the asymmetries of both PLK-1 and CDC-25.1 are lost in each of these *par* mutants, with AB and P1 cells showing equivalent distributions (Fig. 4).

Although PLK-1 and CDC-25 levels are equalized in AB and P1 cells in *par* mutants, we observed differences in staining intensity between them. We compared immunoflourescence intensities of cytoplasmic PLK-1 and nuclear CDC-25.1 in the mutants to those in wild-type AB and P1 cells to gain a qualitative measure of differences in levels. We found that cytoplasmic PLK-1 levels in both AB and P1 cells of *par-3* mutant embryos are similar to those found in wild-type P1 cells (Fig. 5 A and Table S1 C). Similarly, the nuclear levels of CDC-25.1 in AB and P1 cells of *par-3* mutants resemble the low level of wild-type P1 cells (Fig. 5 B and Table S1 D). In contrast, cytoplasmic PLK-1 and nuclear CDC-25.1 are high in both cells of *par-1*, *-2*, and *-4* mutant embryos, similar to wild-type AB cells (Fig. 5, A and B; and Table S1, C and D). These observations suggest that PAR-1, -2, and -4 inhibit and PAR-3 promotes nuclear CDC-25.1 levels, possibly through regulation of PLK-1 abundance.

If the PLK-1 and CDC-25.1 levels are relevant to cell cycle timing, then cell cycle length should be decreased in mutants with increased PLK-1 levels and increased in mutants with lower PLK-1 levels. To test this hypothesis, we measured cell cycle lengths of the synchronous second division in *par-1* mutant and *par-3* mutant embryos and compared them to those of wild-type AB and P1 cells (Table S1 B). In *par-1* mutant embryos, where PLK-1 and CDC-25.1 levels are both high, AB and P1 cells have a fast cell cycle length similar to that of a wild-type AB cell (Fig. 2 B). In *par-3* mutant embryos, where PLK-1 and CDC-25.1 levels are both low, AB and P1 cells have a slow cell cycle length similar to that of a wild-type P1 cell (Fig. 2 B). These results support the view that PAR proteins control cell cycle length through regulation of PLK-1 and CDC-25.1 levels.

A suggestion for how the polarity machinery might regulate PLK-1 and/or CDC-25.1 comes from work on *mex-5* and *mex-6*, two downstream targets of the *par* genes. MEX-5 and MEX-6 are nearly identical functionally redundant CCCH finger proteins that link PAR asymmetries to downstream protein asymmetries (Schubert et al., 2000; DeRenzo et al., 2003). Although their mechanism of action is unknown, they activate cullin-dependent degradation of germplasm proteins in the anterior of the one-cell embryo and in somatic cells such as AB, which leads to asymmetric protein distributions (Schubert et al., 2000; DeRenzo et al., 2003). Interestingly, *mex-5; mex-6* double mutants exhibit a synchronous cell division phenotype at the two-cell stage (Piano et al., 2002). These findings make MEX-5 and MEX-6 good candidates for linking PAR proteins to regulation of PLK-1 and CDC-25.1 asymmetries. If MEX-5 and MEX-6 link PAR function to cell cycle asynchrony, then they would be expected to control the asymmetric distribution of PLK-1 and CDC-25.1. Consistent with this idea, we found that *mex-5(RNAi); mex-6(RNAi)* embryos lack asymmetry of both PLK-1 and CDC-25.1 (Fig. 4). Similar to *par-3* mutants, *mex-5(RNAi); mex-6(RNAi)* embryos show low cytoplasmic PLK-1 levels and low nuclear levels of CDC-25.1 (Fig. 5, A and B; and Table S1, C and D). Intriguingly, MEX-5 and MEX-6 localize asymmetrically to the anterior cytoplasm of the one cell embryo in a pattern similar to that of PLK-1, and this asymmetry is controlled by PAR proteins (Schubert et al., 2000).

Our results support a model whereby the PAR and MEX-5/MEX-6 proteins direct anterior enrichment of PLK-1 at the one-cell stage, and this leads to higher nuclear enrichment of CDC-25.1 in AB at the two-cell stage. The asymmetric localization of these known positive regulators of the cell cycle would result in AB dividing before P1. Loss of either PLK-1 or CDC-25.1 results in a slowing of division in both AB and P1, illustrating the need for both of these components to promote cell division in the two-cell embryo.

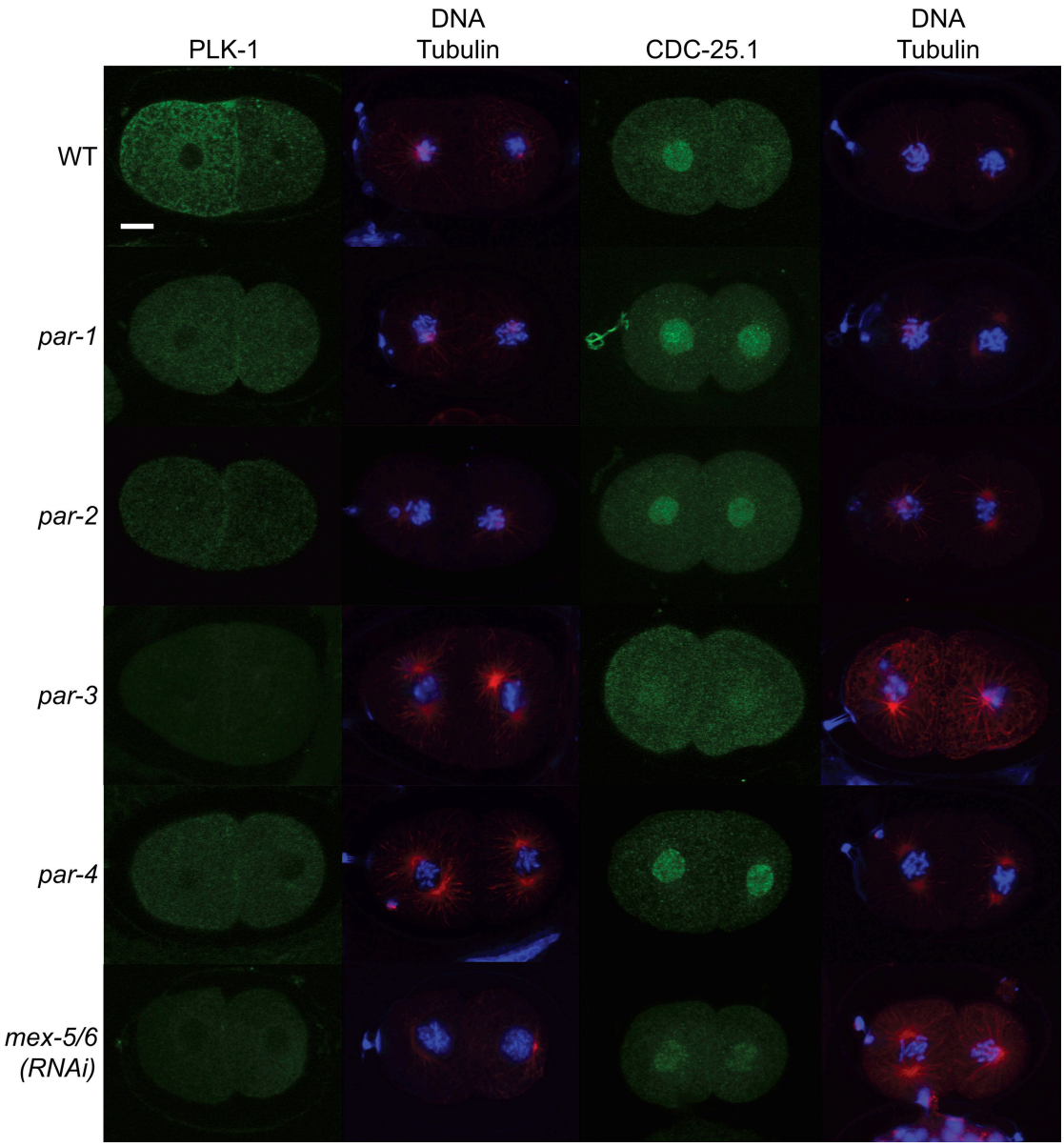

Figure 4. **PLK-1 and CDC-25.1 asymmetries depend on PAR and MEX-5/MEX-6 proteins.** PLK-1 and CDC-25.1 in two-cell embryos (left); and DNA (DAPI, blue) and tubulin (red; right). Cytoplasmic PLK-1 and nuclear CDC-25.1 show symmetric distributions in each mutant. *par-3* mutant and *mex-5; mex-6* double RNAi embryos show low cytoplasmic PLK-1 and nuclear CDC-25.1 levels and *par-1*, *-2*, and *-4* embryos show high cytoplasmic PLK-1 and nuclear CDC-25.1 levels. Quantification is shown in Fig. 5. Bar, 10 μm.

How might the PLK-1 asymmetry be generated? We found that the MEX-5 and MEX-6 proteins, which are downstream targets of the PAR proteins, are required for PLK-1 asymmetry. MEX-5 and MEX-6 activate cullin-dependent protein degradation of germplasm components in AB cells, and this degradation is counteracted in P1 cells by the PAR-1 kinase (DeRenzo et al., 2003). This suggests that the PAR proteins and MEX-5/MEX-6 may generate anterior enrichment of PLK-1 through asymmetric control of PLK-1 levels. Because MEX-5/MEX-6 activates protein degradation in the anterior, though PLK-1 levels appear lower and not higher in *mex-5(RNAi); mex-6(RNAi)* embryos, PLK-1 seems unlikely to be a direct target. Instead, we suggest that MEX-5 and MEX-6 may activate anterior degradation of a yet-to-be-identified negative regulator of PLK-1 levels, leading to anterior stability of PLK-1. PAR-1, which counteracts MEX-5/MEX-6–dependent protein degradation at the posterior, might protect such a factor at the posterior.

These findings may shine light on previous studies that have linked the asynchronous second division in *C. elegans* to DNA replication control (Encalada et al., 2000; Brauchle et al., 2003). DIV-1, which encodes a subunit of the DNA polymerase α-primase complex, is an essential DNA replication factor required for normal division timing in the early *C. elegans* embryo. AB and P1 divisions are both delayed in *div-1* mutants; however, P1 is delayed to a much greater extent, which suggests a link between DNA replication and asynchronous cell division (Encalada et al., 2000). Further support for such a link was provided by a study of the ataxia telangiectasia and Rad3

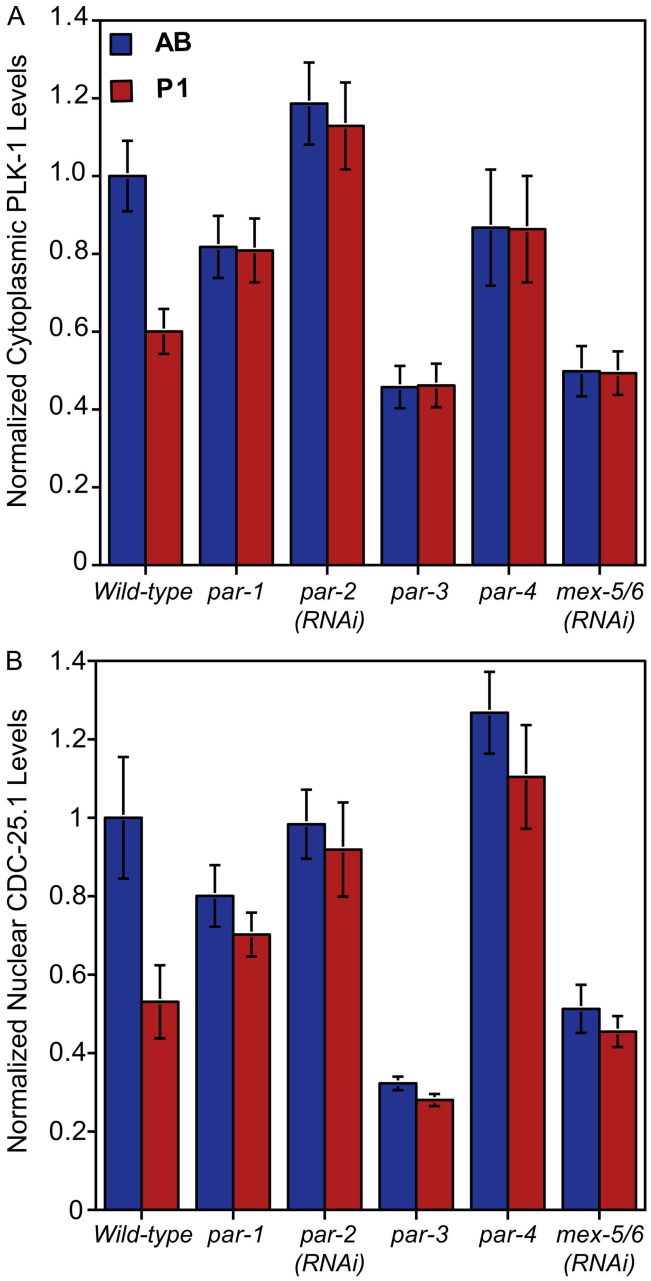

Figure 5. **PLK-1 and CDC-25.1 levels in *par* mutants.** Normalized fluorescent intensities in AB and P1 for cytoplasmic PLK-1 (A) and nuclear CDC-25.1 (B) immunostained wild-type, *par-1*, *par-2(RNAi)*, *par-3*, *par-4*, and *mex-5/mex-6(RNAi)* two-cell embryos. Normalized means ± SEM shown. Corresponding p-values are given in Table S2 (C and D, available at http://wwws.jcb.org/cgi/content/full/jcb.200710018/DC1).

related–like kinase ATL-1 and the CHK1-like kinase CHK-1; these proteins slow both AB and P1 division times, again with a preferential effect in P1. In mammalian cells, Cdc25 and Plk1 have been found to be direct targets of the replication checkpoint (Smits et al., 2000; Bartek et al., 2004; van Vugt et al., 2004; van Vugt and Medema, 2005). We found that lowering embryonic PLK-1 and CDC-25.1 levels affects P1 cell cycle length more than that of AB. Therefore, if the DNA replication checkpoint negatively regulated PLK-1 and/or CDC-25.1 in *C. elegans* embryos, it would be expected to have a larger effect in P1 than in AB even if the checkpoint was symmetrically activated in the two cells. A model consistent with these data are that asymmetric distributions of PLK-1 and CDC-25.1 are the primary regulatory events controlling asynchronous cell cycle timing, and that symmetric action of the DNA replication checkpoint on PLK-1 and/or CDC-25.1 increases asynchrony of cell division. Future studies on these proteins will be needed to test these hypotheses.

In summary, our studies have provided a clear model for differential control of cell cycle length at the two-cell stage: the polarity machinery generates asymmetry of the Polo-like kinase PLK-1 between AB and P1, and this in turn leads to differential accumulation of CDC-25.1 in the nucleus. We suggest that regulation of Polo kinase activity or levels could be a general mechanism for controlling cell cycle length, as Polo kinases are highly regulated enzymes (van Vugt and Medema, 2005; van de Weerdt and Medema, 2006). During development of all animals, cell cycle lengths become different, and this is usually linked with fate determination. An interesting future avenue of study would be to investigate whether there are developmental changes in Polo kinase levels in cells of distinctly different fates and whether or not those levels are critical in fate determination.

Materials and methods

Strains

C. elegans strains were maintained using standard methods (Brenner, 1974). The following strains were used this study: N2, KK288 [*sqt-3(sc8) par-1(b274)*IV/*nT1(unc-?(n754)let-?)* (IV;V)] (Kemphues et al., 1988), JA1438 [*dpy-1(e1) par-2(lw32)/sC1*], KK571 [*lon-1(e185) par-3(it71)/qC1*] (used for immunofluorescence experiments; Cheng et al., 1995), KK653 [*unc-32(e189) par-3(it71)/qC1*] (used for cell cycle timing experiments; Tsou et al., 2002) and KK300 [*par-4(it57ts)*] (Morton et al., 1992).

To generate the GFP::CDC-25.1 animals, the full-length genomic fragment of CDC-25.1, comprising the first ATG to the predicted stop, was gateway cloned into pID3.01 (a gift from G. Seydoux, Howard Hughes Medical Institute, Johns Hopkins University School of Medicine, Baltimore, MD). Simple arrays were generated by coinjection of the GFP::CDC-25.1 construct (5 µg/ml) together with the dominant *rol-6(su1006)* plasmid pRF4 (100 µg/ml) and single-stranded oligonucleotides (1 mg/ml) to facilitate integration (Mello et al., 1991). No integrants were obtained. Four extrachromosomal lines showed GFP::CDC-25.1 expression in the germline and early embryo similar to that of endogenous CDC-25.1 for more than six generations before being silenced.

Immunostaining

Antibody staining of embryos was performed as described previously (Andrews and Ahringer, 2007) using rabbit anti-CDC-25.1(Ashcroft et al., 1999), rabbit anti–PLK-1 (both gifts of A. Golden, National Institutes of Health, Bethesda, MD; Chase et al., 2000), mouse anti–CYE-1(a gift of E. Kiproes, University of Georgia, Athens, GA; Brodigan et al., 2003), and mouse anti-tubulin (DM1A1; Sigma-Aldrich) primary antibodies and Alexa A488 and A594 secondary antibodies (Invitrogen). Embryos were imaged using a 63× objective (Carl Zeiss, Inc.) on a microscope (Axioplan 2; Carl Zeiss, Inc.) fitted with a confocal detection system (LSM 510 Meta; Carl Zeiss, Inc.). Secondary processing of images was performed using Photoshop CS3 and Illustrator CS3 (Adobe).

Single confocal images of wild-type and mutant two-cell embryos immunostained with CDC-25.1 or PLK-1 were taken. Quantification of nuclear and cytoplasmic fluorescent levels were measured using identical circular region of interest positioned within the AB and P1 nuclei or in the AB and P1 cytoplasm as indicated (Metamorph; MDS Analytical Technologies). All values were normalized to the mean of wild-type AB cytoplasmic or nuclear levels and standard errors determined. p-values were calculated using the *t* test.

RNAi

RNAi of *cdc-25.1* and *plk-1* was performed by feeding young adult hermaphrodites RNAi bacterial clones (sjj_K06A5.7 for *cdc-25.1* and sjj_K06H7.1 for *plk-1*) as described previously (Kamath et al., 2003; Ahringer, 2006). *cdc-25.1(RNAi)* embryos were analyzed 18–20 h after feeding at 20°C; these conditions lead to 100% embryonic lethality (n = 92). *plk-1(RNAi)* embryos were analyzed 18–20 h after feeding at 15°C; this causes >99% embryo lethality (n = 142). We observed that PLK-1 levels drop in both AB and P1 after RNAi depletion at 16, 18, and 20 h, with the asymmetry still apparent (Fig. S1). For simultaneous RNAi of *mex-5* and *mex-6*, double-stranded RNA corresponding to each gene was generated using (sjj_W02A2.7 and for *mex-5* sjj_AH6.5 for *mex-6*) the T7 Ribomax RNA kit (Promega), pooled, and injected into young adult hermaphrodites (0.25 mg/ml each). Embryos were analyzed 36 h after injection at 20°C.

Differential interference contrast (DIC), GFP, and FRAP videos

To determine AB and P1 cell cycle lengths, 4D DIC movies of early embryos were made at 20°C, taking 12 z sections at 10-s intervals using a 63× objective on a compound microscope (DMRE; Leica) fitted with a digital camera (ORCA-ER; Hamamatsu) and running Openlab software (Improvision) as described previously (Zipperlen et al., 2001). AB and P1 cell cycle lengths were determined by measuring the time of onset of NEBD in the P0 cell to the onset of NEBD in AB or P1. For each set of experiments, movies of wild-type controls were collected on the same days as the mutant or RNAi embryos to control for environmental variations.

Movies of GFP::CDC-25.1 were made using an LSM 510 Meta confocal microscope. Image capture of 10 z sections of GFP::CDC-25.1 and DIC was performed every 29 s for the non-FRAP videos and every 11 s for the FRAP videos. For the FRAP videos, a non-FRAP time point was taken before the simultaneous bleaching of both AB and P1 nuclei (488 nm laser, 100% power, 200 iterations). All embryos survived to at least the four-cell stage.

Image analysis of the non-FRAP and FRAP videos was performed using the Metamorph software. We measured the fluorescence intensity of a single projected image generated from the three middle planes of both the AB and P1 nuclei for each time point. Identical circular region of interests were positioned within the AB and P1 nuclei and in the AB and P1 cytoplasm and measurements were taken for each time point. Nuclear measurements were corrected for photobleaching with the cytoplasmic fluorescent values. All intensity values were then normalized to the initial intensity value measured at AB for each all the embryos analyzed. The results were plotted using Cricket Graph III (Computer Associates).

Online supplemental material

Fig. S1 is a time course of PLK-1 immunostaining after RNAi depletion of *plk-1* and CDC-25.1 immunostaining after *cdc-25.1* RNAi depletion. Table S1 contains data corresponding to Figs. 2 and 5. Video 1 is a movie of a wild-type GFP::CDC-25.1 two-cell embryo. Video 2 is a FRAP movie of a wild-type GFP::CDC-25.1 two-cell embryo. Online supplemental material is available at http://www.jcb.org/cgi/content/full/jcb.200710018/DC1.

We thank G. Seydoux, A. Golden, and E. Kipreos for providing plasmids and antibodies and B. Fievet, J. Rodriguez, K. Lewis, R. Basto, and I. Latorre for comments on the manuscript. We also thank M. Gotta for help in the initial stages of the project. Some strains used in this work were provided by the Caenorhabditis Genetics Center, which is funded by the National Institutes of Health National Center for Research Resources.

J. Ahringer and D.M. Rivers are supported by a Wellcome Trust Senior Research Fellowship (054523).

Submitted: 2 October 2007
Accepted: 5 February 2008

References

Ahringer, J. 2006. Reverse Genetics. *Wormbook*, editor. The *C. elegans* Research Community, Wormbook, doi/10.1895/wormbook.1.47.1, http://www.wormbook.org.

Andrews, R., and J. Ahringer. 2007. Asymmetry of early endosome distribution in *C. elegans* embryos. *PLoS ONE.* 2:e493.

Ashcroft, N.R., M.E. Kosinski, D. Wickramasinghe, P.J. Donovan, and A. Golden. 1998. The four cdc25 genes from the nematode *Caenorhabditis elegans*. *Gene.* 214:59–66.

Ashcroft, N.R., M. Srayko, M.E. Kosinski, P.E. Mains, and A. Golden. 1999. RNA-mediated interference of a cdc25 homolog in *Caenorhabditis elegans* results in defects in the embryonic cortical membrane, meiosis, and mitosis. *Dev. Biol.* 206:15–32.

Bartek, J., C. Lukas, and J. Lukas. 2004. Checking on DNA damage in S phase. *Nat. Rev. Mol. Cell Biol.* 5:792–804.

Brauchle, M., K. Baumer, and P. Gonczy. 2003. Differential activation of the DNA replication checkpoint contributes to asynchrony of cell division in *C. elegans* embryos. *Curr. Biol.* 13:819–827.

Brenner, S. 1974. The genetics of *Caenorhabditis elegans*. *Genetics.* 77:71–94.

Brodigan, T.M., J. Liu, M. Park, E.T. Kipreos, and M. Krause. 2003. Cyclin E expression during development in *Caenorhabditis elegans*. *Dev. Biol.* 254:102–115.

Busino, L., M. Chiesa, G.F. Draetta, and M. Donzelli. 2004. Cdc25A phosphatase: combinatorial phosphorylation, ubiquitylation and proteolysis. *Oncogene.* 23:2050–2056.

Chase, D., C. Serafinas, N. Ashcroft, M. Kosinski, D. Longo, D.K. Ferris, and A. Golden. 2000. The polo-like kinase PLK-1 is required for nuclear envelope breakdown and the completion of meiosis in *Caenorhabditis elegans*. *Genesis.* 26:26–41.

Cheng, N.N., C.M. Kirby, and K.J. Kemphues. 1995. Control of cleavage spindle orientation in *Caenorhabditis elegans*: the role of the genes par-2 and par-3. *Genetics.* 139:549–559.

Deppe, U., E. Schierenberg, T. Cole, C. Krieg, D. Schmitt, B. Yoder, and G. von Ehrenstein. 1978. Cell lineages of the embryo of the nematode *Caenorhabditis elegans*. *Proc. Natl. Acad. Sci. USA.* 75:376–380.

DeRenzo, C., K.J. Reese, and G. Seydoux. 2003. Exclusion of germ plasm proteins from somatic lineages by cullin-dependent degradation. *Nature.* 424:685–689.

Edgar, L.G., and J.D. McGhee. 1988. DNA synthesis and the control of embryonic gene expression in *C. elegans*. *Cell.* 53:589–599.

Encalada, S.E., P.R. Martin, J.B. Phillips, R. Lyczak, D.R. Hamill, K.A. Swan, and B. Bowerman. 2000. DNA replication defects delay cell division and disrupt cell polarity in early *Caenorhabditis elegans* embryos. *Dev. Biol.* 228:225–238.

Gönczy, P., and L. Rose. 2006. Asymmetric cell division and axis formation in the embryo. *Wormbook*, editor. The *C. elegans* Research Community, Wormbook, doi/10.1895/wormbook.1.47.1, http://www.wormbook.org.

Kalogeropoulos, N., C. Christoforou, A.J. Green, S. Gill, and N.R. Ashcroft. 2004. chk-1 is an essential gene and is required for an S-M checkpoint during early embryogenesis. *Cell Cycle.* 3:1196–1200.

Kamath, R.S., A.G. Fraser, Y. Dong, G. Poulin, R. Durbin, M. Gotta, A. Kanapin, N. Le Bot, S. Moreno, M. Sohrmann, et al. 2003. Systematic functional analysis of the *Caenorhabditis elegans* genome using RNAi. *Nature.* 421:231–237.

Karlsson, C., S. Katich, A. Hagting, I. Hoffmann, and J. Pines. 1999. Cdc25B and Cdc25C differ markedly in their properties as initiators of mitosis. *J. Cell Biol.* 146:573–584.

Kemphues, K.J., J.R. Priess, D.G. Morton, and N.S. Cheng. 1988. Identification of genes required for cytoplasmic localization in early *C. elegans* embryos. *Cell.* 52:311–320.

McGarrity, T.J., and C. Amos. 2006. Peutz-Jeghers syndrome: clinicopathology and molecular alterations. *Cell. Mol. Life Sci.* 63:2135–2144.

Mello, C.C., J.M. Kramer, D. Stinchcomb, and V. Ambros. 1991. Efficient gene transfer in *C.elegans*: extrachromosomal maintenance and integration of transforming sequences. *EMBO J.* 10:3959–3970.

Moroy, T., and C. Geisen. 2004. Cyclin E. *Int. J. Biochem. Cell Biol.* 36:1424–1439.

Morton, D.G., J.M. Roos, and K.J. Kemphues. 1992. par-4, a gene required for cytoplasmic localization and determination of specific cell types in *Caenorhabditis elegans* embryogenesis. *Genetics.* 130:771–790.

Morton, D.G., D.C. Shakes, S. Nugent, D. Dichoso, W. Wang, A. Golden, and K.J. Kemphues. 2002. The *Caenorhabditis elegans* par-5 gene encodes a 14-3-3 protein required for cellular asymmetry in the early embryo. *Dev. Biol.* 241:47–58.

Nance, J. 2005. PAR proteins and the establishment of cell polarity during *C. elegans* development. *Bioessays.* 27:126–135.

Piano, F., A.J. Schetter, D.G. Morton, K.C. Gunsalus, V. Reinke, S.K. Kim, and K.J. Kemphues. 2002. Gene clustering based on RNAi phenotypes of ovary-enriched genes in *C. elegans*. *Curr. Biol.* 12:1959–1964.

Schneider, S.Q., and B. Bowerman. 2003. Cell polarity and the cytoskeleton in the *Caenorhabditis elegans* zygote. *Annu. Rev. Genet.* 37:221–249.

Schubert, C.M., R. Lin, C.J. de Vries, R.H. Plasterk, and J.R. Priess. 2000. MEX-5 and MEX-6 function to establish soma/germline asymmetry in early *C. elegans* embryos. *Mol. Cell.* 5:671–682.

Smits, V.A., R. Klompmaker, L. Arnaud, G. Rijksen, E.A. Nigg, and R.H. Medema. 2000. Polo-like kinase-1 is a target of the DNA damage checkpoint. *Nat. Cell Biol.* 2:672–676.

Sulston, J.E., E. Schierenberg, J.G. White, and J.N. Thomson. 1983. The embryonic cell lineage of the nematode *Caenorhabditis elegans*. *Dev. Biol.* 100:64–119.

Sumiyoshi, E., A. Sugimoto, and M. Yamamoto. 2002. Protein phosphatase 4 is required for centrosome maturation in mitosis and sperm meiosis in *C. elegans*. *J. Cell Sci.* 115:1403–1410.

Toyoshima-Morimoto, F., E. Taniguchi, and E. Nishida. 2002. Plk1 promotes nuclear translocation of human Cdc25C during prophase. *EMBO Rep.* 3:341–348.

Tsou, M.F., A. Hayashi, L.R. DeBella, G. McGrath, and L.S. Rose. 2002. LET-99 determines spindle position and is asymmetrically enriched in response to PAR polarity cues in *C. elegans* embryos. *Development.* 129:4469–4481.

van de Weerdt, B.C., and R.H. Medema. 2006. Polo-like kinases: a team in control of the division. *Cell Cycle.* 5:853–864.

van Vugt, M.A., and R.H. Medema. 2005. Getting in and out of mitosis with Polo-like kinase-1. *Oncogene.* 24:2844–2859.

van Vugt, M.A., B.C. van de Weerdt, G. Vader, H. Janssen, J. Calafat, R. Klompmaker, R.M. Wolthuis, and R.H. Medema. 2004. Polo-like kinase-1 is required for bipolar spindle formation but is dispensable for anaphase promoting complex/Cdc20 activation and initiation of cytokinesis. *J. Biol. Chem.* 279:36841–36854.

Watts, J.L., B. Etemad-Moghadam, S. Guo, L. Boyd, B.W. Draper, C.C. Mello, J.R. Priess, and K.J. Kemphues. 1996. par-6, a gene involved in the establishment of asymmetry in early *C. elegans* embryos, mediates the asymmetric localization of PAR-3. *Development.* 122:3133–3140.

Watts, J.L., D.G. Morton, J. Bestman, and K.J. Kemphues. 2000. The *C. elegans* par-4 gene encodes a putative serine-threonine kinase required for establishing embryonic asymmetry. *Development.* 127:1467–1475.

Zipperlen, P., A.G. Fraser, R.S. Kamath, M. Martinez-Campos, and J. Ahringer. 2001. Roles for 147 embryonic lethal genes on *C.elegans* chromosome I identified by RNA interference and video microscopy. *EMBO J.* 20:3984–3992.